Free Radical Biology and Medicine 53 (2012) 1770–1781

Contents lists available at SciVerse ScienceDirect

Free Radical Biology and Medicine

journal homepage: www.elsevier.com/locate/freeradbiomed

Original Contributions

Phloretin ameliorates 2-chlorohexadecanal-mediated brain microvascular endothelial cell dysfunction in vitro

Andreas Üllen [a], Günter Fauler [b], Eva Bernhart [a], Christoph Nusshold [a], Helga Reicher [a], Hans-Jörg Leis [c], Ernst Malle [a], Wolfgang Sattler [a,*]

[a] Institute of Molecular Biology and Biochemistry, University Children's Hospital, Medical University of Graz, Graz, Austria
[b] Clinical Institute of Medical and Chemical Laboratory Diagnostics, University Children's Hospital, Medical University of Graz, Graz, Austria
[c] Research Unit of Osteology and Analytical Mass Spectrometry, University Children's Hospital, Medical University of Graz, 8010 Graz, Austria

ARTICLE INFO

Article history:
Received 21 September 2011
Received in revised form
11 June 2012
Accepted 18 August 2012
Available online 25 August 2012

Keywords:
Chlorinative stress
Hypochlorite
Myeloperoxidase
2-ClHDA
Blood–brain barrier
Free radicals

ABSTRACT

2-Chlorohexadecanal (2-ClHDA), a chlorinated fatty aldehyde, is formed via attack on ether-phospholipids by hypochlorous acid (HOCl) that is generated by the myeloperoxidase–hydrogen peroxide–chloride system of activated leukocytes. 2-ClHDA levels are elevated in atherosclerotic lesions, myocardial infarction, and neuroinflammation. Neuroinflammatory conditions are accompanied by accumulation of neutrophils (an ample source of myeloperoxidase) in the brain. Microvessel damage by inflammatory mediators and/or reactive oxidants can induce blood–brain barrier (BBB) dysfunction, a pathological condition leading to cerebral edema, brain hemorrhage, and neuronal death. In this in vitro study we investigated the impact of 2-ClHDA on brain microvascular endothelial cells (BMVEC), which constitute the morphological basis of the BBB. We show that exogenously added 2-ClHDA is subject to rapid uptake and metabolism by BMVEC. Using C16 structural analogues of 2-ClHDA we found that the cytotoxic potential decreases in the following order: 2-ClHDA > hexadecanal > palmitic acid > 2-ClHDA-dimethylacetal. 2-ClHDA induces loss of barrier function, mitochondrial dysfunction, apoptosis via activation of caspase 3, and altered intracellular redox balance. Finally we investigated potential protective effects of several natural polyphenols on in vitro BBB function. Of the compounds tested, phloretin almost completely abrogated 2-ClHDA-induced BMVEC barrier dysfunction and cell death. These data suggest that 2-ClHDA has the potential to induce BBB breakdown under inflammatory conditions and that phloretin confers protection in this experimental setting.

composition as a
lative stress are
ed disorders and

cells (BMVEC) form the physical basis of the blood–brain barrier (BBB) by the formation of tight and adherens junction complexes [2]. These complexes prevent paracellular transport of molecules and cells, thereby maintaining brain homeostasis via elaborately regulated transport mechanisms [1,3]. However, inflammatory processes, including endothelial transmigration of leukocytes and activation of glial cells and subsequent production of inflammatory mediators and/or reactive oxygen species (ROS), can induce BBB permeability and amplify neurodegeneration [4]. Dysfunctional mitochondria, amyloid-β peptides, redox-active iron, and the NADPH-oxidase complex are potential sources of reactive species at the neurovasculature and in deeper brain regions [5,6].

injury [5]. Within the cerebral lipid subclasses ether-phospholipids (predominantly plasmalogens) take a central structural and functional role in brain function [7]. Plasmalogen deficiency results in severe and long-lasting developmental alterations of the cerebellum [8], and decreased plasmalogen content is linked to neurodegenerative diseases [9,10].

During activation of phagocytes the myeloperoxidase (MPO)–H_2O_2–chloride system contributes to oxidant generation [11,12]. Increasing evidence points toward MPO as a disease-amplifying enzyme in neurodegeneration [6]. In multiple sclerosis, MPO is present in microglia/macrophages at lesion sites [13,14]. Cortical demyelination is associated with increased MPO activity [15,16] and neuroinflammation increases cerebral MPO levels [17]. 2-Chlorohexadecanal (2-ClHDA) is a naturally occurring chlorinated fatty aldehyde generated by HOCl-targeting of the vinyl-ether bond of plasmalogens. 2-ClHDA is generated by activated neutrophils [18,19] and monocytes [20] and concentrations are

* Corresponding author. Fax: +43 316 380 9615.
E-mail address: wolfgang.sattler@medunigraz.at (W. Sattler).

0891-5849
http://dx.doi.org/10.1016/j.freeradbiomed.2012.08.575

elevated in human atherosclerotic lesions [21], ischemic/reperfused myocardium [22], and inflamed brain tissue [17]. 2-ClHDA is a potent neutrophil chemoattractant [19] and a potent inhibitor of vasculoprotective endothelial nitric oxide synthase (eNOS) [18].

Neutrophils immobilize and kill invading microbes extracellularly through the formation of neutrophil extracellular traps (NETs) [23]. During this process, termed NETosis, neutrophil MPO synergizes with elastase in promoting chromatin decondensation and NET formation [24]. Neutrophils are able to produce and secrete chlorinated lipids [25]. Thus it is possible that the MPO–H_2O_2–chloride system leads to modification and/or chlorination of the endogenous neutrophil plasmalogen pool that could amplify modification of extracellular targets at the BBB.

Oxidative stress contributes to BBB dysfunction in neurodegenerative diseases. One potential contributor in this setting is neutrophil- or glia-derived MPO that is capable of oxidatively targeting plasmalogens [19,20], thereby generating chlorinated lipids including 2-ClHDA. This study aimed to elucidate the impact of exogenously added 2-ClHDA on BMVEC metabolic activity and function (mitochondrial and endothelial barrier function). To pursue potential pharmacotherapeutic applications, naturally occurring polyphenols were tested for their potential to ameliorate lipotoxic effects displayed by 2-ClHDA.

Materials and methods

Materials

Cell culture supplies were from Gibco (Vienna, Austria), PAA Laboratories (Linz, Austria), Costar (Vienna, Austria), or VWR (Austria). Dulbecco's modified Eagle's medium (DMEM) Ham's F12 and hydrocortisone were from Sigma–Aldrich (Vienna, Austria). Electrical cell-substrate impedance sensing (ECIS) electrode arrays (8W10E+) were from Ibidi (Martinsried, Germany). Dimethyl sulfoxide (DMSO), sodium hypochlorite (NaOCl), 3-(4,5-dimethyl-2-thiazolyl)-2,5-diphenyltetrazolium bromide (MTT), palmitic acid, colchicine, apigenin, curcumin, genistein, naringenin, phloretin, phloridzin, resveratrol, *N,N*-diisopropylethylamine, pentadecanoic acid, pentadecanol, heptadecanoic acid, dipalmitoylphosphatidylcholine, glycerol tripalmitate, cholesteryl palmitate, *N*-acetylcysteine (NAC), pentafluorobenzyl (PFB) hydroxylamine, PFB bromide, and pentafluorobenzoyl (PFBoyl) were from Sigma–Aldrich. Silica gel 60 plates were from Merck (Darmstadt, Germany). Staurosporine was from Calbiochem (La Jolla, CA, USA). 5-(And-6)-carboxy-2′,7′-dichlorodihydrofluorescein diacetate (carboxy-H_2DCFDA) and 5,5′,6,6′-tetrachloro-1,1′,3,3′-tetraethylbenzimidazolylcarbocyanine iodide (JC-1) were from Molecular Probes (Invitrogen, Vienna, Austria). Phenylmethylsulfonyl fluoride (PMSF), aprotinin, leupeptin, and pepstatin were from Sigma–Aldrich. Polyvinylidene difluoride (PVDF) transfer membrane (Biotrace PVDF) was from Pall Corp. (Vienna, Austria). Detergents and other chemicals were from Sigma–Aldrich. ECL SuperSignal Western blotting substrate was obtained from Pierce (Rockford, IL, USA) and CURIX Ultra UV-G X-ray films were from Agfa (Mortsel, Belgium). Polyclonal rabbit anti-human caspase 3 antibody was from Santa Cruz Biotechnology (Santa Cruz, CA, USA) and horseradish peroxidase-conjugated goat anti-rabbit IgG was from Pierce. All other chemicals and solvents were from Sigma–Aldrich or Roth (Vienna, Austria).

Isolation and culture of primary porcine brain microvascular endothelial cells

BMVEC were isolated from porcine brains obtained from the local slaughterhouse by a combination of mechanical disintegration, enzymatic digestion, and centrifugation steps [26]. After removal of meninges and the secretory areas, the brain cortex (gray and white matters) was minced using a sterile cutter with staggered rolling blades. Minced tissue was suspended in "preparation medium" (M199 supplemented with penicillin/streptomycin (P/S; 100 μg/ml), gentamycin (100 μg/ml), and glutamine (0.68 mM)) and incubated with solid dispase (0.1%, w/v) for 1 to 2 h at 37 °C in a water bath with gentle stirring. Dextran solution (16%, w/v) was added to get a final 10% (w/v) dextran suspension followed by centrifugation at 6800 *g* for 10 min at 4 °C. The resulting pellet was resuspended in "medium A" (M199 supplemented with P/S (100 μg/ml), gentamycin (100 μg/ml), and glutamine (0.68 mM, and 10% ox serum)). Larger vessels were separated by a filtration step through a 180-μm nylon mesh. Microvessels were digested with 0.03% (w/v) collagenase/dispase for 5 min at 37 °C in a water bath with gentle stirring. After collection of released BMVEC aggregates by low-spin centrifugation at 140 *g* for 10 min at room temperature (RT) they were further purified by density gradient centrifugation. Cells obtained from one brain were resuspended in 5 ml medium A and centrifuged on a discontinuous Percoll gradient (20 ml 1.03 g/ml bottom-layered with 15 ml 1.07 g/ml) at 1300 *g* for 10 min at RT in a swinging bucket rotor without brake. BMVEC clusters, which were gathered at the interface of the two phases, were washed in medium A and plated onto six to eight 75 cm^2 collagen-coated culture flasks. After 1 day in culture the cells were washed twice with phosphate-buffered saline (PBS) and cultivated in "medium B" (medium A without gentamycin).

After 2 to 3 days, when confluence was almost reached, BMVEC were subcultured by trypsinization and seeded onto collagen-coated cell culture ware (6-, 12-, 24-, and 96-well plates, 60 μg/ml collagen in PBS) or onto ECIS arrays (200 μg/ml collagen in 150 mM NaCl) at densities between 20,000 (multiwell plates) and 40,000 cells/cm^2 (ECIS arrays).

Determination of NaOCl concentration

The concentration of NaOCl (termed reagent HOCl) was determined for each experiment using the molar absorption coefficient for NaOCl of 350 cm^{-1} at 292 nm at pH 12. Dilutions of NaOCl were prepared in Milli-Q water.

Cell experiments

Before starting cell culture experiments BMVEC were preincubated overnight with serum-free medium B. For ECIS experiments medium B was replaced by "induction medium" (DMEM Ham's F12 medium supplemented with P/S (100 μg/ml), glutamine (0.68 mM), and hydrocortisone (500 nM; to induce formation of tight junctions)). During cell experiments BMVEC were incubated in serum-free medium B or induction medium in the absence or presence of 2-ClHDA, reagent HOCl, structural analogues of 2-ClHDA (palmitic acid, hexadecanal (HDA), and 2-ClHDA-dimethylacetal (dma)), polyphenols, or inducers of apoptosis (staurosporine and colchicine; 1 μM each) for the indicated time periods. Freshly deprotected 2-ClHDA and HDA as well as other structural analogues of 2-ClHDA, polyphenols, and staurosporine were prepared as stock solutions in DMSO. For each cell experiment using 2-ClHDA (or structural analogues) the final concentration of DMSO in the medium was 0.4% (v/v). Reagent HOCl and colchicine were prepared as 250× stock solutions in water.

Electrical cell-substrate impedance sensing

To determine the effects of 2-ClHDA and phloretin on barrier function, impedance measurement was performed using an ECIS

Z System (Applied Biophysics, Troy, NY, USA). BMVEC were plated on collagen-coated gold electrodes of 8W10E+ arrays and impedance was recorded in real time at 1-min intervals at 4 and 64 kHz. After induction of tight junctions by hydrocortisone the average baseline impedance readings varied between 2000 and 5000 Ω at 4 kHz and between 600 and 800 Ω at 64 kHz. Experiments were started when a stable basal impedance of $>2000\ \Omega$ at 4 kHz was obtained.

MTT test

To investigate the effects of 2-ClHDA, structural analogues of 2-ClHDA, and reagent HOCl on BMVEC metabolic activity in the absence or presence of polyphenols the MTT test was used [27]. BMVEC were grown in 12-, 24-, or 96-well plates to confluence and treated with 2-ClHDA or reagent HOCl in serum-free medium B at the indicated concentrations and for the indicated time periods. In the case of cotreatment, cells were preincubated with polyphenols at the indicated concentrations for 30 min before addition of 2-ClHDA. After treatment, the medium was replaced by serum-free medium (100–500 μl per well) containing MTT (1.2 mM) and the cells were incubated for 1 h under standard conditions. The cells were washed (PBS) and lysed (isopropanol/1 M HCl, 25/1 (v/v); 100 μl) on a rotary shaker (1000 rpm, 15 min). Absorbance was measured at 570 nm on a Victor 1420 multilabel counter (Wallac) and corrected for background absorption (650 nm).

JC-1 assay

To examine the mitochondrial membrane potential ($\Delta\psi m$) of BMVEC after treatment with 2-ClHDA or reagent HOCl, the JC-1 assay was performed [28]. Cells were grown to confluence in black 96-well plates (Greiner, Linz, Austria) before 2-ClHDA or reagent HOCl was added in serum-deprived medium at the indicated concentrations and for the indicated time periods. Cells were then incubated with JC-1 (10 μM, added to serum-free medium B as 2 mM stock solution in DMSO, 100 μl per well) at 37 °C in the dark for 90 min followed by two washing steps with PBS. Fifty microliters of PBS was then added to each well and fluorescence intensities were read at 485/535 nm (excitation/emission) for detection of the green substrate and 544/590 nm (excitation/emission) for detection of the red substrate using a Victor 1420 multilabel counter.

Measurement of carboxy-H_2DCFDA oxidation

After internalization and subsequent hydrolysis the redox indicator probe carboxy-H_2DCFDA is converted to carboxy-H_2DCF, which, in the presence of oxidant species, undergoes oxidation to the fluorescent carboxy-DCF [29]. BMVEC were grown to confluence in six-well plates before the cells were incubated with H_2DCFDA dissolved in PBS (10–25 μM, added as 300× stock solution in DMSO) for 1 h at 37 °C in the dark. Subsequently, PBS was replaced by serum-free medium B containing the indicated concentrations of 2-ClHDA and the cells were incubated at 37 °C in the dark. Incubations were stopped by washing the cells two times with ice-cold PBS and, then, the plates were kept on ice for 10 min. Cell lysis was performed with 300 μl lysis solution (3% Triton X-100 in PBS) on a rotary shaker (1350 rpm) at 4 °C in the dark for 60 min. Afterward, 50 μl EtOH was added to each well and shaking was continued for another 15 min to ensure complete solubilization of deacetylated and oxidized DCF. The cell lysates were transferred to Eppendorf tubes and centrifuged to remove cellular debris (13,000 rpm, 4 °C, 10 min). Two hundred microliters of the supernatant were transferred to black 96-well microtiter plates and fluorescence intensity was measured at 485/535 nm (excitation/emission) on a Victor 1420 multilabel counter. An aliquot of the supernatant was used to determine the protein concentration using the BCA assay. To investigate whether DCF fluorescence is sensitive toward altered intracellular thiol content, BMVEC were incubated in the presence of NAC (5 mM, 1 h) followed by the addition of 2-ClHDA (25 μM, 3 h).

Analysis of (pro)caspase 3 activation

Western blotting

BMVEC were plated in six-well trays and allowed to grow to confluence. Cells were incubated in the absence or presence of 2-ClHDA, reagent HOCl, colchicine, or staurosporine at the indicated concentrations and for the indicated time periods. For protein isolation, the cells were washed twice with ice-cold PBS and then scraped in 50 μl lysis buffer containing PMSF and 1 μg/ml each aprotinin, leupeptin, and pepstatin. After the cellular debris was removed by centrifugation (13,000 rpm, 4 °C, 10 min) the protein content was determined using the Bradford assay (Bio-Rad). Protein extracts were diluted in sample buffer and heated to 95 °C for 5 min before the proteins were separated by SDS–PAGE (10 or 12% polyacrylamide gels, 150 V). Subsequently, the proteins were electrophoretically transferred to PVDF membranes (150 mA, 45 min). Nonspecific adsorption was blocked by incubation with 5% (w/v) low-fat milk powder in Tris-buffered saline/Tween 20 (TBS-T). Rabbit anti-caspase 3 antibody (diluted 1:400 in 5% low-fat milk in TBS-T) was applied by overnight incubation at 4 °C. Immunoreactive bands were visualized using horseradish peroxidase-conjugated goat anti-rabbit IgG (1:5000 in 5% (w/v) nonfat milk powder in TBS-T, 2 h, RT) and subsequent ECL Super-Signal development.

Caspase 3 activity

BMVEC were cultured to confluence in 24-well plates. Subsequently, the cells were incubated with 2-ClHDA, staurosporine, and/or phloretin in serum-deprived medium at the indicated concentrations for 5 h. Cellular caspase 3 activity was determined using the EnzChek Caspase 3 Assay Kit 2 (Molecular Probes) according to the manufacturer's instructions. The assay is based on rhodamine-derived substrate Z-DEVD-R110, which yields a fluorescent product upon proteolytic cleavage by active caspase 3. To confirm that the observed fluorescence signal in induced cells was due to the activity of caspase 3-like proteases the inhibitor Ac-DEVD-CHO was added to cell lysates. Fluorescence intensities were measured at 484/540 nm (excitation/emission) in black 96-well microtiter plates on a Victor 1420 multilabel counter.

Determination of cellular ATP levels

ATP levels of BMVEC were measured using the ATP Determination Kit according to the manufacturer's (Molecular Probes) recommendations. Briefly, BMVEC were cultured to confluence in 96-well plates before 2-ClHDA and/or polyphenols were added in serum-deprived medium at the indicated concentrations. After 5 h the cells were washed twice with PBS and boiled for 5 min in 100 μl of distilled water. Ten microliters of each sample or 10 μl of each dilution for the ATP standard curve (0–5000 nM) were transferred to a well of a 96-well plate before 90 μl of reaction solution was added and mixed. Finally, after a 10-s delay the chemiluminescence was measured on a VICTOR3 multilabel reader (Wallac).

2-ClHDA decay in the cellular supernatant

BMVEC were plated in six-well trays and allowed to grow to confluence. Cells were incubated with 4.1 μg 2-ClHDA (250×

stock solution in DMSO; 10 μM final concentration). At the indicated times lipids from 1 ml of culture medium were extracted twice in 2 ml hexane/methanol (5/1; v/v) in the presence of 100 ng 2-Cl[$^{13}C_8$]HDA as internal standard, which was synthesized as described previously [17]. After conversion to the corresponding PFB-oxime derivatives 2-ClHDA was quantitated by negative-ion chemical ionization gas chromatography mass spectrometry (NICI–GC–MS, see below). A one-phase exponential decay model ($C_t = C_0 \times e^{-kt}$) was used to fit experimental data using Prism 5.0 (GraphPad Software).

Uptake and metabolism of 2-ClHDA by BMVEC

BMVEC plated in six-well trays were grown to confluence. Cells were incubated with 4.1 μg 2-ClHDA for the indicated time periods. Subsequently, lipids from 1 ml of culture medium were extracted twice in 2 ml hexane/methanol (5/1; v/v) in the presence of 2-Cl[$^{13}C_8$]HDA, pentadecanoic acid, and pentadecanol (each 100 ng). Cellular lipids were extracted in the presence of internal standards (100 ng each) using two consecutive extractions (30 min at RT) with 1 ml of hexane/isopropanol (3/2; v/v) on a rotary shaker (1000 rpm). After preparation of PFB-oxime and PFB-ester derivatives, 2-ClHDA, 2-chlorohexadecanoic acid (2-ClHA), and 2-chlorohexadecanol (2-ClHOH) were quantitated by NICI–GC–MS.

2-ClHA distribution in complex lipids

BMVEC plated in petri dishes (10 cm) were grown to confluence (5.5×10^6 cells). Cells were incubated with 17.8 μg 2-ClHDA (250× stock in DMSO; 8 μM, final concentration) for the indicated time periods. Subsequently, cellular lipids were extracted using two consecutive extractions (30 min at RT) with 5 ml of hexane/isopropanol (3/2, v/v) on a rotary shaker (1000 rpm). For isolation of complex lipid fractions cellular lipids were separated on silica gel 60 plates using hexane/diethyl ether/acidic acid (70/30/1, v/v/v) as the mobile phase. Fractions comigrating with dipalmitoylphosphatidylcholine, tripalmitate, and cholesteryl palmitate were scraped off, supplemented with 100 ng heptadecanoic acid as internal standard, and extracted from the TLC sorbent using $CHCl_3$/MeOH (2/1, v/v). For generation of free fatty acids, lipid extracts were dispersed in 500 μl 0.5 M NaOH by sonication and vortexing and incubated for 1 h in a boiling water bath. Subsequently, the samples were cooled to RT, neutralized by addition of 500 μl 0.5 M HCl, and acidified with acetic acid. The released free fatty acids were extracted, converted to the corresponding PFB-esters, and analyzed by NICI–GC–MS.

Derivatization procedures

Preparation of PFB-oxime derivatives of 2-ClHDA was performed as previously described [17]. Fatty acids were converted to the corresponding PFB-ester derivatives in 100 μl 0.35% (v/v) PFB-bromide in acetonitrile and 20 μl *N,N*-diisopropylethylamine for 30 min at RT. Fatty alcohols were converted to PFB-esters using 100 μl 0.4% (v/v) PFBoyl chloride in acetonitrile for 1 h at 80 °C. Derivatization reagents were evaporated on an Eppendorf concentrator. Samples were redissolved in 100 μl hexane, transferred to autosampler vials, and stored at −20 °C until GC–MS analysis.

NICI–GC–MS analysis

Samples were separated on a Thermo Scientific Trace GC Ultra (helium was used as carrier gas, 2 ml/min) with an SGE BPX5 capillary column (15 m, 0.25 mm inner diameter, 0.25 μm methyl silicone film coating) and analyzed using a DSQII mass spectrometer (Thermo Scientific). Injector temperature was set to 230 °C and ion source temperature was 180 °C. The oven temperature was maintained at 100 °C for 5 min, increased during the first ramping step at a rate of 20 °C/min to 175 °C, and held at 175 °C for 1 min. In the second ramping step the temperature was raised at a rate of 15 °C/min to 280 °C and held at 280 °C for an additional 2 min. All spectra were monitored in NICI (methane was used as reagent gas), either in full scan or using selected ion monitoring mode (SIM). In SIM, target compounds were identified at molecule-specific mass-to-charge ratios (Table 1) and the characteristic isotope distribution of chlorine (Cl^{35}/Cl^{37}, 3/1). Quantitation was performed by peak area comparison with internal standards (Table 1).

Table 1
Identification and quantification of analytes by SIM.

Analyte (PFB derivative)	*m/z*	Internal standard (PFB-derivative)	*m/z*	Internal standard (ng)
2-ClHDA	288/290, 414	2-Cl[$^{13}C_8$]HDA	288/290, 422	100
2-ClHA	289/291, 254	Pentadecanoic acid Heptadecanoic acid	241 269	100
2-ClHOH	470/472, 435	Pentadecanol	422	100

Statistical analyses

Data are presented as means ± SD. To test differences in groups, statistical significance was determined by Student's *t* test or one- or two-way ANOVA with Bonferroni correction (using the GraphPad 5.0 Prism package) as indicated. All values of $p \leq 0.05$ were considered significant.

Results

Uptake and metabolism of 2-ClHDA by BMVEC

To test whether 2-ClHDA is taken up by BMVEC, cells were incubated with the aldehyde (15 nmol/well). Cellular and medium lipids were extracted and quantitatively analyzed as PFB-oximes by NICI–GC–MS. 2-ClHDA concentrations in the cellular supernatant were fitted to an exponential decay revealing a half-life of 120 min (Fig. 1A). The decay of 2-ClHDA in the medium was accompanied by a concomitant increase in cellular 2-ClHDA concentrations reaching a maximum of 1 nmol (Fig. 1B; corresponding to approx 7% of 2-ClHDA initially present in the medium) after 120 min.

To get an indication of how 2-ClHDA is metabolized by BMVEC the formation of the redox metabolites [30] 2-ClHOH and 2-ClHA was analyzed by NICI–GC–MS (Figs. 2A and B). Within the first 2 h 2-ClHOH and 2-ClHA accumulated in the cell monolayer at concentrations of 1.9 and 0.4 nmol. Whereas 2-ClHOH concentrations were slightly decreasing at longer time periods, 2-ClHA levels remained constant. Both chlorinated lipids were detectable in the culture medium (approx. 10% of cell-associated 2-ClHOH and 30% of cell-associated 2-ClHA), indicating cellular release of metabolites and/or synthesis via extracellular redox events.

A time course of the precursor (2-ClHDA added at $t=0$)–product relationship (sum of 2-ClHDA, 2-ClHOH, and 2-ClHA in cells and medium, termed 2-ClHX) is shown in Fig. 2C. It is evident that at early time points (up to 60 min) the loss of 2-ClHDA and accumulation of 2-ClHX are equal. Nevertheless

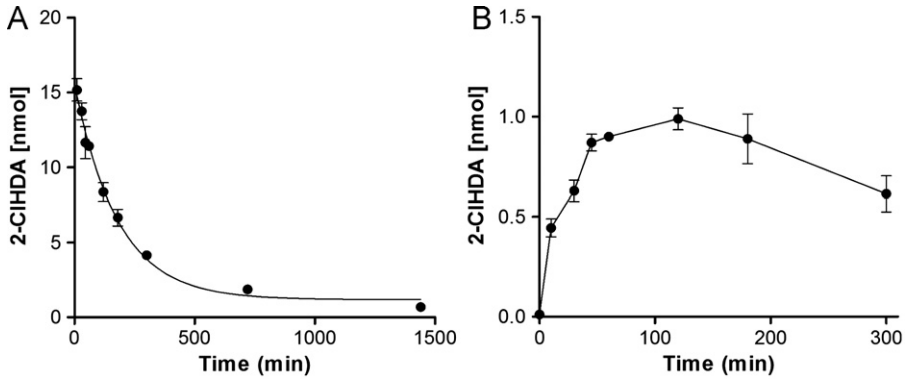

Fig. 1. Uptake kinetics of exogenous 2-ClHDA by BMVEC. Cells (9×10^5) were incubated with 2-ClHDA (stock added in DMSO; final aldehyde concentration 10 μM). At the indicated times, cellular lipids and lipids of the culture medium were extracted in the presence of 100 ng 2-Cl[$^{13}C_8$]HDA. After conversion to the corresponding PFB-oxime derivatives the 2-ClHDA content of (A) the culture medium and (B) BMVEC was quantitated by NICI–GC–MS analysis. Results represent mean values ± SD of three independent experiments. Experimental data of 2-ClHDA decay in the culture medium (A) were fitted by nonlinear regression analysis (R^2=0.98).

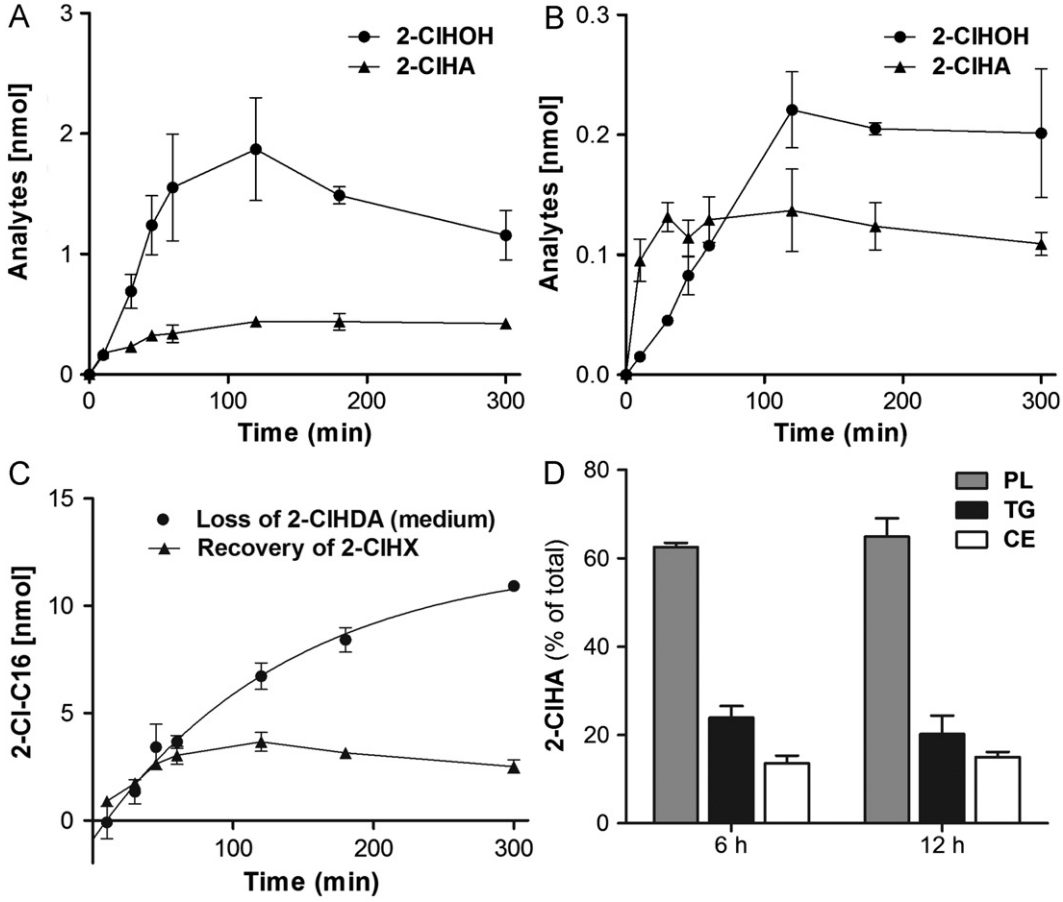

Fig. 2. Metabolism of exogenous 2-ClHDA by BMVEC. Cells (9×10^5) were incubated with 2-ClHDA (stock added in DMSO; final concentration 10 μM). At the indicated times, cellular lipids and lipids of the culture medium were extracted in the presence of pentadecanol and pentadecanoic acid as internal standards. After conversion to PFB-ester derivatives, 2-chlorohexadecanoic acid (2-ClHA) and 2-chlorohexadecanol (2-ClHOH) concentrations were quantitated from (A) cellular and (B) medium lipid extracts by NICI–GC–MS analysis. (C) Loss of 2-ClHDA vs recovery of 2-ClHX (the sum of 2-ClHDA, 2-ClHOH, and 2-ClHA in cells and medium). (D) Cells (5.5×10^6) were incubated with 2-ClHDA (stock added in DMSO; final aldehyde concentration 8 μM). At the indicated times, cellular lipids were extracted. After preseparation of lipid classes by TLC and subsequent extraction from TLC plates, free fatty acids were generated by alkaline hydrolysis. After conversion to the corresponding PFB-ester derivatives, 2-ClHA concentrations were quantitated by NICI–GC–MS with heptadecanoic acid as internal standard. Results represent mean values ± SD of triplicate determinations. PL, phospholipid; TG, triglyceride; CE, cholesteryl ester.

recovery of 2-ClHDA and its metabolites after 5 h accounts for only 25% of total added 2-ClHDA.

One of the pathways contributing to loss of 2-ClHDA is its oxidation to 2-ClHA and subsequent reincorporation into the storage pool of complex lipids [30]. To clarify the ability of BMVEC to form chlorinated complex lipids, cells were incubated in the presence of 2-ClHDA and cellular lipids were preseparated by TLC. Bands comigrating with phospholipids, triglycerides, and cholesteryl

esters were scraped, hydrolyzed, and analyzed by NICI–GC–MS. These experiments revealed that after 6 h approximately 63, 24, and 13% of 2-ClHA was present in the phospholipid, triglyceride, and cholesteryl ester fractions. This percentage distribution remained grossly unchanged after 12 h (Fig. 2D).

2-ClHDA severely impairs metabolic activity of BMVEC

2-ClHDA significantly impaired cellular MTT reduction in a time- and concentration-dependent manner (Fig. 3A) at much lower concentrations compared to reagent HOCl (Fig. 3B). Of note, LC_{50} concentrations of reagent HOCl were approximately 10- to 20-fold higher than for 2-ClHDA. DMSO used as vehicle for 2-ClHDA delivery was without effects on MTT reduction (Supplementary Fig. IA).

Cytotoxic properties have structural specificity

2-ClHDA contains two functional groups attached to an aliphatic chain. To get an indication of the structural requirements that mediate cytotoxicity, three structurally related C16 analogues (Fig. 4A), namely HDA, palmitic acid, and 2-ClHDA-dma, were analyzed for their cytotoxic potential in addition to 2-ClHDA. Cytotoxicity decreased in the order 2-ClHDA > HDA > palmitic acid > 2-ClHDA-dma (Fig. 4B). In these experiments 2-ClHDA reduced metabolic activity by 60 (25 μM) and 90% (50 μM), whereas the nonchlorinated analogue HDA impaired metabolic activity by approximately 40 (25 μM) and 50% (50 μM). Palmitic acid, a fatty acid with potent lipotoxic properties, induced a 20% decrease in MTT reduction at the highest concentration used (50 μM). The chemically inert 2-ClHDA-dma was without effect.

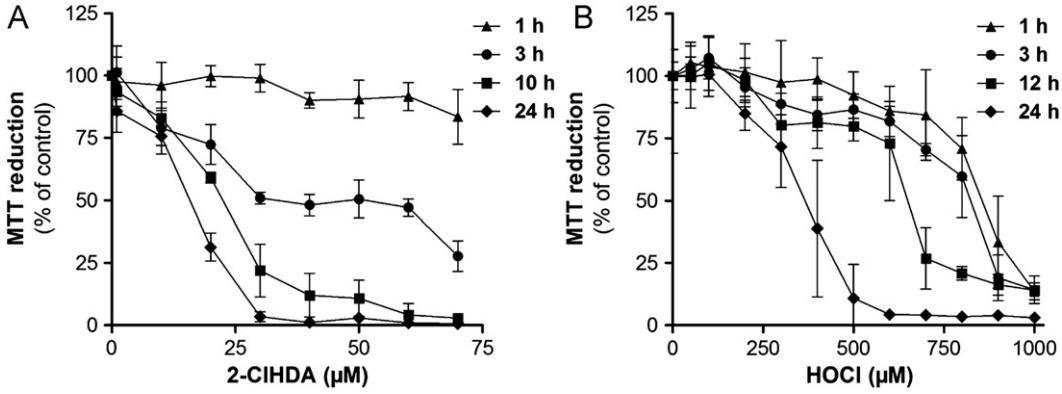

Fig. 3. 2-ClHDA impairs metabolic activity of BMVEC. Cells were incubated in the absence or presence of (A) 2-ClHDA or (B) reagent HOCl at the indicated concentrations for the indicated time periods. Metabolic activity was analyzed by the MTT test. Results are expressed as % of controls and represent mean values ± SD of triplicate (A) or quadruplicate (B) determinations.

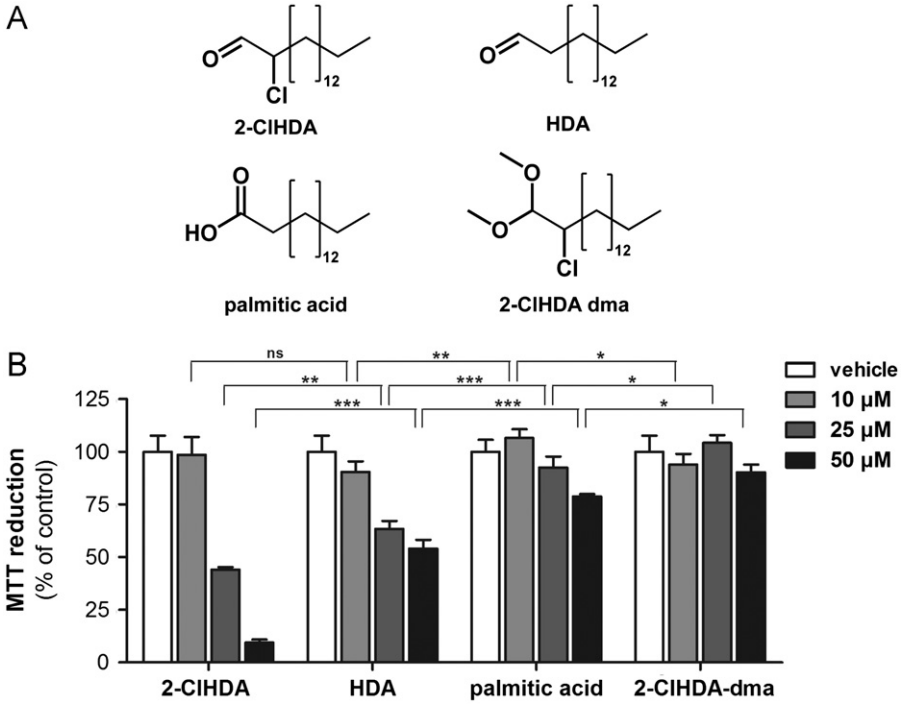

Fig. 4. Cytotoxic potential depends on functional groups. (A) Structures of the four different C16 compounds used in MTT assays. (B) Cells were challenged overnight with the compounds shown in (A). After treatment, BMVEC metabolic activity was analyzed by the MTT test. Results are expressed as % of controls and represent mean values ± SD of triplicate determinations (ns, not significant; $^{*}p < 0.05$, $^{**}p < 0.01$, $^{***}p < 0.001$, two-way ANOVA).

Hence, the presence of a chlorine atom significantly potentiates the cytotoxic properties of HDA, indicating that 2-ClHDA is a mediator with high lipotoxic potential.

2-ClHDA impairs mitochondrial function and induces apoptosis in BMVEC

To determine whether impaired MTT reduction is accompanied by mitochondrial dysfunction $\Delta\psi m$ was analyzed using JC-1 as a fluorophore. DMSO used as vehicle was without effect on $\Delta\psi m$ (Supplementary Fig. IB). Results of these measurements (Figs. 5A and B) revealed that both 2-ClHDA and HOCl impaired $\Delta\psi m$, but with different efficacies: whereas the IC_{50} values for 2-ClHDA were $\approx$ 25, 13, and 5 μM at 1, 3, and 5 h, the corresponding values for reagent HOCl were 500 (3 h) and 350 μM (5 h). Thus after a 5-h incubation 2-ClHDA was 70-fold more efficient in promoting mitochondrial alterations than reagent HOCl.

To establish if 2-ClHDA-mediated mitochondrial dysfunction leads to alterations of intracellular redox balance the redox-sensitive dye carboxy-H_2DCFDA was used. Whereas the vehicle

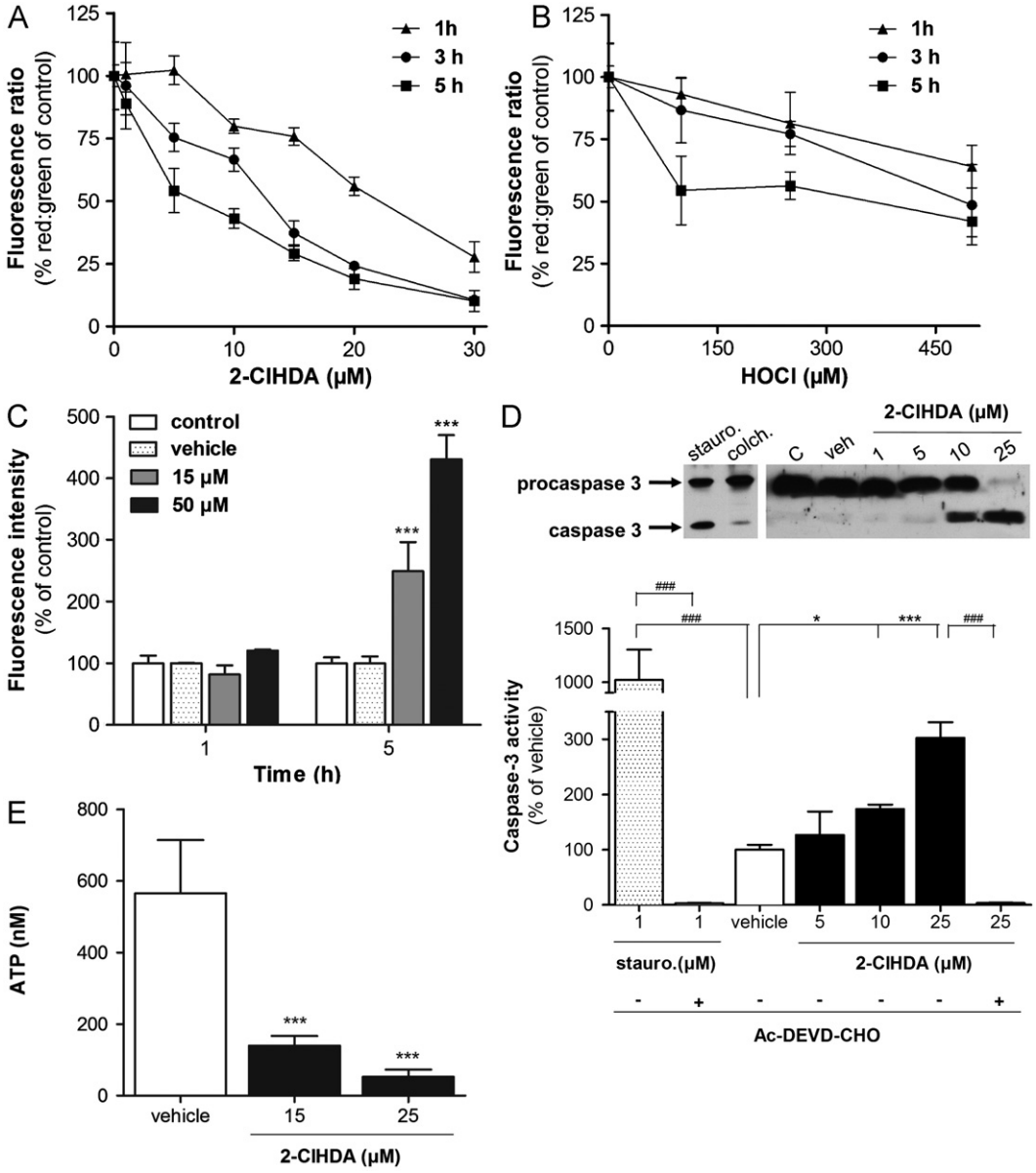

Fig. 5. 2-ClHDA induces mitochondrial dysfunction, increases DCFDA fluorescence, and leads to apoptosis in BMVEC. Cells were incubated in the absence or presence of (A) 2-ClHDA or (B) reagent HOCl at the indicated concentrations for the indicated time periods. After treatment, $\Delta\psi m$ was analyzed using the JC-1 assay. Data were calculated by division of red by green fluorescence. Results are expressed as % of red to green fluorescence ratio compared to controls and represent the means ± SD of three independent experiments. (C) The cellular redox status was determined using the redox-sensitive compound carboxy-H_2DCFDA. Cells were preincubated with nonfluorescent carboxy-H_2DCFDA followed by treatment with 2-ClHDA at the indicated concentrations for the indicated time periods. The fluorescence intensity is expressed as % of control and represents the mean ± SD of three independent experiments ($^{***}p < 0.001$; two-way ANOVA). Control, no addition; vehicle, 0.4% DMSO (v/v). (D) Cells were incubated with 2-ClHDA (5 h) before caspase 3 measurement. Staurosporine (stauro.) and colchicine (colch.) were used as known inducers of apoptosis. Procaspase 3 processing was analyzed using rabbit polyclonal anti-caspase 3 as primary antibody (top). Procaspase 3 (32 kDa) and caspase 3 (17 kDa) were visualized using horseradish peroxidase-conjugated secondary antibody and the ECL system (C, control; veh, vehicle control, DMSO 0.4%). Caspase 3 activity was determined as outlined under Materials and methods. Results represent means ± SD from triplicate determinations ($^{*}p < 0.05$, $^{***}p < 0.001$, two-way ANOVA; $^{\#\#\#}p < 0.001$, Student's *t* test). (E) Cells were incubated with 2-ClHDA (5 h) and intracellular ATP concentrations were analyzed as described under Materials and methods. Results represent means ± SD of four independent experiments ($^{***}p < 0.01$, one way ANOVA).

was without effect, 2-ClHDA increased fluorescence intensity at 15 and 50 μM (Fig. 5C), concentrations that also decreased MTT reduction and mitochondrial function of BMVEC (Fig. 5A). 2-ClHDA caused an increase in DCF-dependent fluorescence that is suggestive of increased ROS production. 2-ClHDA-induced DCFDA conversion was blocked by the thiol-containing antioxidant NAC (Supplementary Fig. II). To investigate whether 2-ClHDA induces apoptosis procaspase 3 activation was analyzed. The known inducers of apoptosis staurosporine and colchicine served as controls. 2-ClHDA concentrations ≥ 5 μM induced procaspase 3 processing (Fig. 5D, top). Concentrations of 5–10 μM induced partial proteolytic cleavage of procaspase 3, and a concentration of 25 μM 2-ClHDA resulted in almost quantitative conversion of procaspase 3 into active caspase 3. This was also reflected by caspase 3 activity measurements (Fig. 5D, bottom): 2-ClHDA at 10 and 25 μM induced caspase 3 activity approximately two- and threefold over vehicle controls. 2-ClHDA- and staurosporine-induced caspase 3 activation was eliminated in the presence of the inhibitor Ac-DEVD-CHO. Mitochondrial function was assessed by measuring cellular ATP concentrations. These analyses revealed that 2-ClHDA severely depleted (70–90%) the cellular ATP pool in comparison to vehicle-treated cells (Fig. 5E).

Screening for cytoprotective polyphenols

Increasing evidence suggests that some members of the flavonoid and nonflavonoid polyphenol family display neuroprotective properties [31,32]. We therefore investigated the effects of representative polyphenols (Supplementary Fig. III) on MTT reduction. Under the experimental conditions applied, apigenin (a flavone), curcumin (a diarylheptanoid), and resveratrol (a stilbenoid) decreased metabolic activity, indicative of mitochondrial dysfunction (Supplementary Fig. IV). The remaining compounds, i.e., genistein (an isoflavone), naringenin (a flavanone), and phloretin (a dihydrochalcone), had either no (except genistein at 100 μM) or beneficial effects. To provide a more direct measure of mitochondrial function we analyzed cellular ATP levels in polyphenol-supplemented BMVEC (Supplementary Fig. V). The most deleterious effects were observed in curcumin-treated cells in which intracellular ATP was almost completely depleted. Apigenin, genistein (at low concentrations), naringenin, and resveratrol were without significant effects, whereas phloretin (and genistein at 100 μM) significantly increased the cellular ATP content (Supplementary Fig. V).

Next, the potential of genistein, naringenin, and phloretin to ameliorate 2-ClHDA-induced cytotoxicity was investigated in more detail. Under the experimental conditions applied genistein (up to 100 μM) had no significant effect on BMVEC survival in the presence of 2-ClHDA (Fig. 6A). Naringenin slightly but significantly increased MTT reduction, whereas phloretin provided the most pronounced protection against 2-ClHDA-induced metabolic dysfunction. Most importantly, phloretin provided protection also at 25 and 50 μM (Fig. 6B).

To get an insight into the structural requirements for cell protection, the efficacy of phloretin was compared with that of its naturally occurring glycosylated dietary precursor phloridzin (for structure see Supplementary Fig. III). In contrast to nonglycosylated phloretin, its glycosylated analogue was without effect or even decreased the metabolic activity of BMVEC (Fig. 6C). These data suggest that the hydroxyl group at C2 of phloretin is probably involved in BMVEC protection against 2-ClHDA cytotoxicity.

Finally we investigated the effects of phloretin on caspase 3 activation and the cellular ATP status in 2-ClHDA-treated cells. Basal caspase 3 activity was unaffected by phloretin alone. However, activity significantly increased in response to 15 μM 2-ClHDA and was reduced to control levels when cells were incubated in the presence of 2-ClHDA and phloretin (Fig. 6D). A similar rescue phenotype was observed for cellular ATP levels: 2-ClHDA reduced cellular ATP concentrations by approximately 80% in comparison to vehicle-treated cells. However, the presence of phloretin had a pronounced protective function and partially preserved the intracellular ATP content (Fig. 6E).

Phloretin restores barrier function of 2-ClHDA-treated BMVEC

To determine the effects of phloretin on 2-ClHDA-mediated barrier dysfunction BMVEC were pretreated with phloretin before challenge with 2-ClHDA and impedance was monitored using the ECIS system. Measuring barrier function (4 kHz) and the integrity of the cell monolayer (64 kHz) revealed that barrier dysfunction was rapidly induced in response to 2-ClHDA (Fig. 7A; the 30-h time point is shown in Fig. 7B). Disruption of the cell monolayer lagged by approximately 2–2.5 h behind (Fig. 7C; 30-h time point is shown in Fig. 7D). 2-ClHDA-induced barrier dysfunction was attenuated by phloretin (Fig. 7A), whereas the integrity of the cell monolayer was almost completely conserved in the presence of phloretin (Fig. 7C).

Phloretin reduces cellular 2-ClHDA content

Phloretin is a nonspecific inhibitor of cellular fatty acid uptake [33]; we have investigated whether it would also interfere with chlorinated fatty aldehyde uptake. Phloretin pretreatment significantly decreased the amount of cell-associated 2-ClHDA at all time points investigated (Fig. 8A); these data suggest inhibition of 2-ClHDA uptake by phloretin. Surprisingly, NICI–GC–MS data also revealed that 2-ClHDA levels in the cellular supernatant supplemented with phloretin were significantly lower compared to controls; again, this effect was time-dependent (Fig. 8B). Whether these observations are due to covalent adduct formation between 2-ClHDA and phloretin is currently under investigation.

Discussion

The findings of this in vitro study strengthen the concept that reactive aldehydes generated under (neuro)inflammatory conditions can induce BBB dysfunction [34]. Our data demonstrate that 2-ClHDA (a fatty aldehyde generated via MPO-specific pathways) impairs metabolic activity, induces mitochondrial dysfunction, and leads to increased DCF-dependent fluorescence being indicative of ROS generation in primary BMVEC. In addition, 2-ClHDA potently induces apoptosis at concentrations that are present in human atherosclerotic lesion material [21] and in brains of mice with endotoxin-induced neuroinflammation [17]. Our finding that phloretin alleviates 2-ClHDA-induced barrier dysfunction could have therapeutic potential in a setting in which BBB function is compromised under conditions of oxidative/chlorinative stress.

Results of this study demonstrate that BMVEC actively metabolize 2-ClHDA to 2-ClHOH and 2-ClHA. This pathway was shown to depend on fatty aldehyde dehydrogenase (ALDH3A2) activity [25] in coronary artery endothelial cells [30]. ALDH3A2 deficiency results in ichthyosis, spastic paraplegia, and mental retardation probably due to abnormal membrane lipid accumulation in skin and brain and formation of Schiff's base adducts with lipids and/or proteins [35]. The precursor–product analyses performed during this study revealed that only 25% of initially added chlorinated fatty aldehyde was recovered as 2-ClHDA, 2-ClHOH, or 2-ClHA. There are several plausible explanations for this loss: (i) 2-ClHA is incorporated into the complex lipid fraction (Fig. 2D), (ii) 2-ClHDA is able to form Schiff's base adducts with ethanolamine-containing glycerophospholipids and/or the ε-amino group of protein lysine

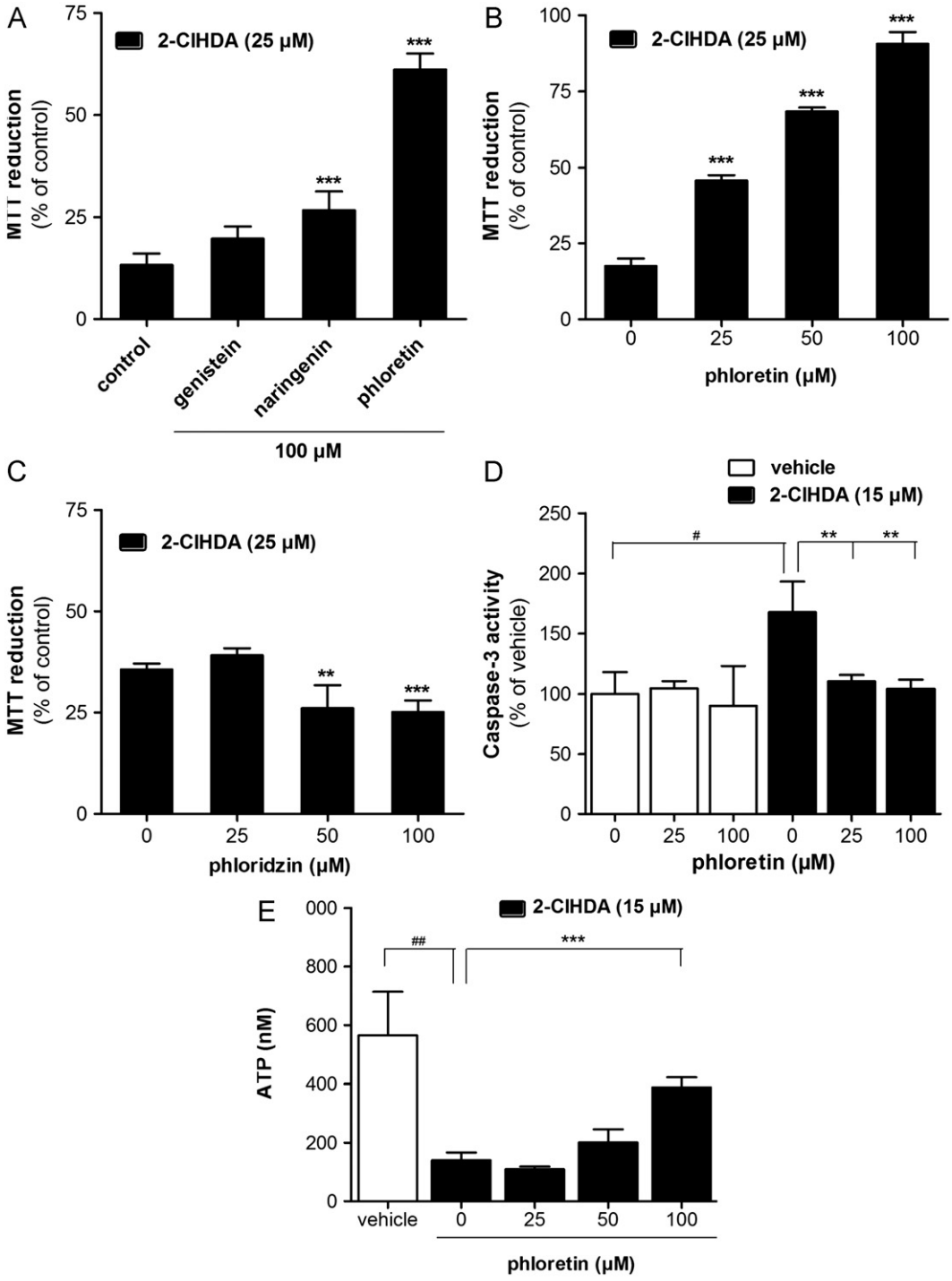

Fig. 6. Impact of selected polyphenols on 2-ClHDA-induced cell death in BMVEC. Cells were preincubated in the presence of the indicated concentrations of genistein, naringenin, phloretin, or phloridzin. After an incubation in the presence of 2-ClHDA MTT tests were performed after (A) 16 or (B, C) 5 h. Results are expressed as % of controls and represent mean values ± SD of quadruplicate determinations ($^{**}p < 0.01$, $^{***}p < 0.001$, one-way ANOVA). (D) Basal and 2-ClHDA-induced (5 h) caspase 3 activity was measured in the absence or presence of the indicated phloretin concentrations. DMSO (0.4%) was used as vehicle control. Results are expressed as % of controls and represent mean values ± SD of triplicate determinations ($^{**}p < 0.01$, one way ANOVA; $^{\#}p < 0.05$, Student's *t* test). (E) After an incubation with vehicle (DMSO, 0.4%) or 2-ClHDA in the absence or presence of indicated phloretin concentrations cellular ATP concentrations were quantitated. Results represent mean values ± SD of triplicate determinations ($^{***}p < 0.001$, one-way ANOVA; $^{\#\#}p < 0.05$, Student's *t* test).

residues [36,37], and (iii) 2-ClHA is subject to ω- and subsequent β-oxidation starting at the ω-carboxylic acid function [38].

Of note, the ω-oxidation pathway is also active in brain [39], although it is not clear whether brain-derived metabolites accumulate in cerebrospinal fluid or the peripheral circulation. ω-Oxidation of chlorinated fatty aldehydes may also be active in the cerebrovasculature: this is supported by data demonstrating that BMVEC are able to oxidize 20-hydroxyeicosatetraenoic acid to 20-carboxyeicosatetraenoic acid and chain-shortened β-oxidation-derived dicarboxylic acid metabolites [40].

With regard to the MTT results, 2-ClHDA displayed higher cytotoxicity toward BMVEC compared to reagent HOCl and structurally related C16 analogues (Figs. 3 and 4). Because of relatively low target selectivity it might be reasonable to assume that a major

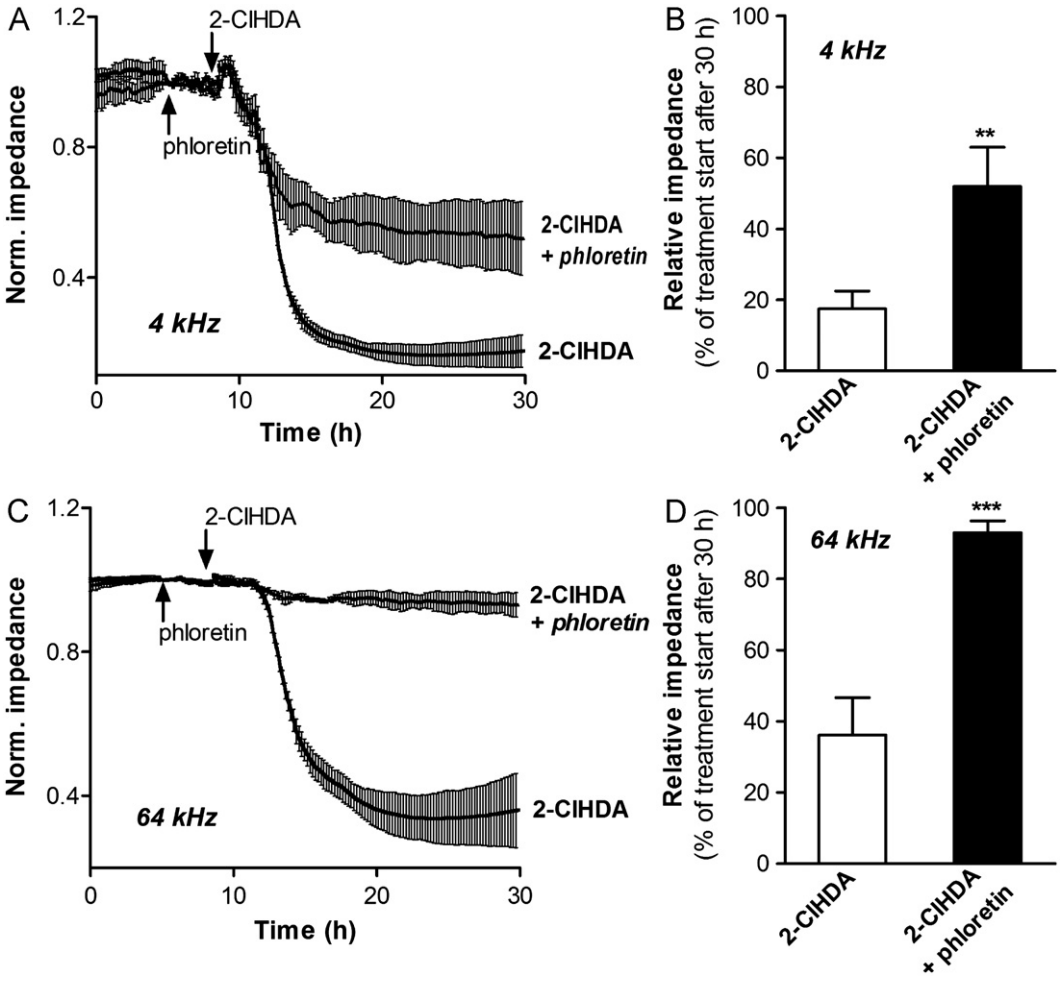

Fig. 7. Phloretin rescues barrier function of 2-ClHDA-treated BMVEC. Cells were plated on gold microelectrodes and cultured to confluence. Impedance of hydrocortisone-induced monolayers (7.5×10^4 cells) was continuously monitored at (A) 4 kHz and (C) 64 kHz. The corresponding 30-h time points are shown in (B) and (D). After stabilization, cells were pretreated with 100 μM phloretin or vehicle for 3 h and then challenged with 25 μM 2-ClHDA. Impedance values were normalized to treatment start and represent mean values ± SD of four independent experiments ($^{**}p < 0.01$, $^{***}p < 0.001$, Student's t test).

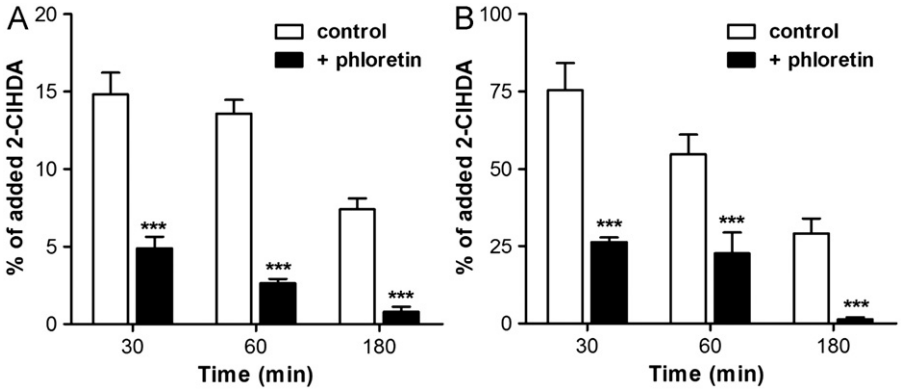

Fig. 8. Phloretin reduces intra- and extracellular 2-ClHDA levels in BMVEC cultures. After pretreatment with phloretin (100 μM, 1 h) cells (9×10^5) were incubated with 25 μM 2-CHDA. At the indicated times cellular lipids and lipids of the cellular supernatant were extracted. After conversion to PFB-oxime derivatives 2-ClHDA concentrations in (A) cellular and (B) medium lipid extracts were quantitated by NICI–GC–MS analysis. Results are expressed as % of added 2-ClHDA and represent mean values ± SD of triplicate determinations ($^{***}p < 0.001$, two-way ANOVA).

fraction of HOCl is consumed during modification of putative targets at the extrafacial leaflet of the plasma membrane. The cytotoxic properties of C16 analogues decreased in the order 2-ClHDA > HDA > palmitic acid > 2-ClHDA-dma (Fig. 4). In a manner similar to that observed here, 2-iodohexadeacanal (the major iodolipid in thyroid gland [41]) but not hexadecanal inhibited cell proliferation in a rat model of goiter [42]. Chlorinated lipids are potent signaling mediators: 2-ClHDA activates COX-2 [43] and is an inhibitor of eNOS biosynthesis [18]. Interestingly, a structural analogue of 2-ClHDA, 2-bromopalmitate, is a potent inhibitor of protein acylation, a key event targeting eNOS to the Golgi complex and cholesterol-rich microdomains of the plasma membranes [44].

Emerging evidence suggests that mitochondrial dysfunction plays a major role in neurological disorders such as Alzheimer disease, multiple sclerosis, Parkinson disease, and stroke [45]. It is well established that electrophilic lipids, such as 4-hydroxy-2-nonenal, the cyclopentenone 15-deoxy-$\Delta^{12,14}$-prostaglandin J_2, and 15-J_2-isoprostane, induce ROS formation in endothelial cells, most probably because of direct interaction with mitochondria and/or alterations of the intracellular redox balance [46]. These pathophysiological conditions might have particularly deleterious consequences on transport systems at the BBB. BMVEC have a high density of mitochondria, which reflects the energy demand necessary to fuel the elaborately developed (ATP-dependent) transport systems present at either the luminal or the abluminal side of the BBB [1]. During normal oxidative phosphorylation electrons leak out of the electron transport chain, giving rise to the formation of superoxide anions, an event that might be prevalent at the BBB. Superoxide anions are generated at both, complex I (NADH dehydrogenase) and complex III (ubiquinone Q-cytochrome *b*) and alterations in the redox status of these enzyme complexes result in excessive production of ROS [47]. Subsequent dismutation of superoxide anion radical to H_2O_2 could further fuel the MPO–H_2O_2–chloride system.

Endothelial barrier modulation by reactive aldehydes includes Michael adduct formation, increased protein tyrosine phosphorylation, redox-dependent mechanisms due to thiol depletion and/or mitochondrial dysfunction, reorganization of the endothelial cytoskeleton, and integrin-based events [48] or activation of matrix metalloproteinases [49]. In human BMVEC cultures it was demonstrated that Cyp2E1-dependent oxidation of ethanol to acetic aldehyde results in ROS production, subsequent activation of myosin light-chain kinase, phosphorylation of tight-junction proteins, increased endothelial permeability, and enhanced monocyte migration across the BBB [50]. In a guinea pig model of neurotoxicity increased 4-hydroxy-2-nonenal formation was accompanied by altered distribution of the tight-junction-associated proteins zonula occludens-1 and claudin-5 [51].

One of the major findings obtained here is a potent rescue capacity of the dihydrochalcone-type polyphenol phloretin. Phloretin is a nonspecific fatty acid uptake inhibitor at the BBB [52]. Our data suggest that phloretin could also interfere with 2-ClHDA uptake by BMVEC, thereby attenuating adverse effects. Among the various polyphenols investigated, phloretin effectively suppressed cytotoxicity and barrier dysfunction (Figs. 6 and 7), observations in line with our preliminary hypothesis that phloretin inhibits cellular 2-ClHDA-mediated uptake. However, 2-ClHDA concentrations in the cellular supernatant were also significantly lower compared to incubations in the absence of phloretin. This observation raises the possibility that phloretin could form covalent adducts with the chlorinated aldehyde. Phloridzin, the glucoside of phloretin, was without beneficial effects on BMVEC, suggesting that 2-ClHDA trapping is specific to phloretin. The underlying mechanisms are currently unclear and under investigation by our group.

In conclusion, the results of this study demonstrate that 2-ClHDA has deleterious effects on BMVEC function, indicating that activation of neutrophils and subsequent release of 2-ClHDA could contribute to BBB dysfunction under pathological conditions. Findings that phloretin potently ameliorates these adverse effects opens potentially new pharmacotherapeutical strategies to interfere with aldehyde-mediated BBB dysfunction.

Acknowledgments

Financial support was provided by the Austrian Science Fund (FWF; Grants F3007 and P19074-B05), the Austrian Nationalbank (Anniversary Fund, Project 14534), and the Austrian Research Promotion Agency (Grant Bridge P820107). A.Ü. and C.N. were funded by the FWF within the Ph.D. program Molecular Medicine of the Medical University of Graz.

Appendix A. Supplementary material

Supplementary data associated with this article can be found in the online version at http://dx.doi.org/10.1016/j.freeradbiomed.2012.08.575.

References

[1] Zlokovic, B. V. The blood–brain barrier in health and chronic neurodegenerative disorders. *Neuron* **57:**178–201; 2008.
[2] Hawkins, B. T.; Davis, T. P. The blood–brain barrier/neurovascular unit in health and disease. *Pharmacol. Rev.* **57:**173–185; 2005.
[3] Pardridge, W. M. Blood–brain barrier delivery. *Drug Discovery Today* **12:** 54–61; 2007.
[4] Coisne, C.; Engelhardt, B. Tight junctions in brain barriers during central nervous system inflammation. *Antioxid. Redox Signaling* **15:**1285–1303; 2011.
[5] Halliwell, B. Oxidative stress and neurodegeneration: where are we now? *J. Neurochem.* **97:**1634–1658; 2006.
[6] Yap, Y. W.; Whiteman, M.; Cheung, N. S. Chlorinative stress: an under appreciated mediator of neurodegeneration? Cell *Signalling* **19:**219–228; 2007.
[7] Gorgas, K.; Teigler, A.; Komljenovic, D.; Just, W. W. The ether lipid-deficient mouse: tracking down plasmalogen functions. *Biochim. Biophys. Acta* **1763:**1511–1526; 2006.
[8] Teigler, A.; Komljenovic, D.; Draguhn, A.; Gorgas, K.; Just, W. W. Defects in myelination, paranode organization and Purkinje cell innervation in the ether lipid-deficient mouse cerebellum. *Hum. Mol. Genet.* **18:**1897–1908; 2009.
[9] Goodenowe, D. B.; Cook, L. L.; Liu, J.; Lu, Y.; Jayasinghe, D. A.; Ahiahonu, P. W.; Heath, D.; Yamazaki, Y.; Flax, J.; Krenitsky, K. F.; Sparks, D. L.; Lerner, A.; Friedland, R. P.; Kudo, T.; Kamino, K.; Morihara, T.; Takeda, M.; Wood, P. L. Peripheral ethanolamine plasmalogen deficiency: a logical causative factor in Alzheimer's disease and dementia. *J. Lipid Res.* **48:**2485–2498; 2007.
[10] Han, X. Multi-dimensional mass spectrometry-based shotgun lipidomics and the altered lipids at the mild cognitive impairment stage of Alzheimer's disease. *Biochim. Biophys. Acta* **1801:**774–783; 2010.
[11] Klebanoff, S. J. Myeloperoxidase: friend and foe. *J. Leukocyte Biol.* **77:**598–625; 2005.
[12] Malle, E.; Furtmuller, P. G.; Sattler, W.; Obinger, C. Myeloperoxidase: a target for new drug development? Br *J. Pharmacol* **152:**838–854; 2007.
[13] Nagra, R. M.; Becher, B.; Tourtellotte, W. W.; Antel, J. P.; Gold, D.; Paladino, T.; Smith, R. A.; Nelson, J. R.; Reynolds, W. F. Immunohistochemical and genetic evidence of myeloperoxidase involvement in multiple sclerosis. *J. Neuroimmunol.* **78:**97–107; 1997.
[14] Chen, J. W.; Breckwoldt, M. O.; Aikawa, E.; Chiang, G.; Weissleder, R. Myeloperoxidase-targeted imaging of active inflammatory lesions in murine experimental autoimmune encephalomyelitis. *Brain* **131:**1123–1133; 2008.
[15] Gray, E.; Thomas, T. L.; Betmouni, S. Scolding, N.; Love, S. Elevated activity and microglial expression of myeloperoxidase in demyelinated cerebral cortex in multiple sclerosis. *Brain Pathol.* **18:**86–95; 2008.
[16] Marik, C.; Felts, P. A.; Bauer, J.; Lassmann, H.; Smith, K. J. Lesion genesis in a subset of patients with multiple sclerosis: a role for innate immunity? *Brain* **130:**2800–2815; 2007.
[17] Ullen, A.; Fauler, G.; Kofeler, H.; Waltl, S.; Nusshold, C.; Bernhart, E.; Reicher, H.; Leis, H. J.; Wintersperger, A.; Malle, E.; Sattler, W. Mouse brain plasmalogens are targets for hypochlorous acid-mediated modification in vitro and in vivo. *Free Radic. Biol. Med.* **49:**1655–1665; 2010.
[18] Marsche, G.; Heller, R.; Fauler, G.; Kovacevic, A.; Nuszkowski, A.; Graier, W.; Sattler, W.; Malle, E. 2-Chlorohexadecanal derived from hypochlorite-modified high-density lipoprotein-associated plasmalogen is a natural inhibitor of endothelial nitric oxide biosynthesis. *Arterioscler. Thromb. Vasc. Biol.* **24:**2302–2306; 2004.
[19] Thukkani, A. K.; Hsu, F. F.; Crowley, J. R.; Wysolmerski, R. B.; Albert, C. J.; Ford, D. A. Reactive chlorinating species produced during neutrophil activation target tissue plasmalogens: production of the chemoattractant, 2-chlorohexadecanal. *J. Biol. Chem.* **277:**3842–3849; 2002.
[20] Thukkani, A. K.; Albert, C. J.; Wildsmith, K. R.; Messner, M. C.; Martinson, B. D.; Hsu, F. F.; Ford, D. A. Myeloperoxidase-derived reactive chlorinating species from human monocytes target plasmalogens in low density lipoprotein. *J. Biol. Chem.* **278:**36365–36372; 2003.
[21] Thukkani, A. K.; McHowat, J.; Hsu, F. F.; Brennan, M. L.; Hazen, S. L.; Ford, D. A. Identification of alpha-chloro fatty aldehydes and unsaturated lysophosphatidylcholine molecular species in human atherosclerotic lesions. *Circulation* **108:**3128–3133; 2003.
[22] Thukkani, A. K.; Martinson, B. D.; Albert, C. J.; Vogler, G. A.; Ford, D. A. Neutrophil-mediated accumulation of 2-ClHDA during myocardial infarction:

2-ClHDA-mediated myocardial injury. *Am. J. Physiol. Heart Circ. Physiol* **288:**H2955–H2964; 2005.
[23] Villanueva, E.; Yalavarthi, S.; Berthier, C. C.; Hodgin, J. B.; Khandpur, R.; Lin, A. M.; Rubin, C. J.; Zhao, W.; Olsen, S. H.; Klinker, M.; Shealy, D.; Denny, M. F.; Plumas, J.; Chaperot, L.; Kretzler, M.; Bruce, A. T.; Kaplan, M. J. Netting neutrophils induce endothelial damage, infiltrate tissues, and expose immunostimulatory molecules in systemic lupus erythematosus. *J. Immunol.* **187:**538–552; 2011.
[24] Papayannopoulos, V.; Metzler, K. D.; Hakkim, A.; Zychlinsky, A. Neutrophil elastase and myeloperoxidase regulate the formation of neutrophil extracellular traps. *J. Cell Biol.* **191:**677–691; 2010.
[25] Anbukumar, D. S.; Shornick, L. P.; Albert, C. J.; Steward, M. M.; Zoeller, R. A.; Neumann, W. L.; Ford, D. A. Chlorinated lipid species in activated human neutrophils: lipid metabolites of 2-chlorohexadecanal. *J. Lipid Res.* **51:**1085–1092; 2010.
[26] Goti, D.; Hammer, A.; Galla, H. J.; Malle, E.; Sattler, W. Uptake of lipoprotein-associated alpha-tocopherol by primary porcine brain capillary endothelial cells. *J. Neurochem.* **74:**1374–1383; 2000.
[27] Kratzer, I.; Wernig, K.; Panzenboeck, U.; Bernhart, E.; Reicher, H.; Wronski, R.; Windisch, M.; Hammer, A.; Malle, E.; Zimmer, A.; Sattler, W. Apolipoprotein A-I coating of protamine-oligonucleotide nanoparticles increases particle uptake and transcytosis in an in vitro model of the blood–brain barrier. *J. Controlled Release* **117:**301–311; 2007.
[28] Nusshold, C.; Kollroser, M.; Kofeler, H.; Rechberger, G.; Reicher, H.; Ullen, A.; Bernhart, E.; Waltl, S.; Kratzer, I.; Hermetter, A.; Hackl, H.; Trajanoski, Z.; Hrzenjak, A.; Malle, E.; Sattler, W. Hypochlorite modification of sphingomyelin generates chlorinated lipid species that induce apoptosis and proteome alterations in dopaminergic PC12 neurons in vitro. *Free Radic. Biol. Med.* **48:**1588–1600; 2010.
[29] Halliwell, B.; Whiteman, M. Measuring reactive species and oxidative damage in vivo and in cell culture: how should you do it and what do the results mean? *Br. J. Pharmacol.* **142:**231–255; 2004.
[30] Wildsmith, K. R.; Albert, C. J.; Anbukumar, D. S.; Ford, D. A. Metabolism of myeloperoxidase-derived 2-chlorohexadecanal. *J. Biol. Chem.* **281:**16849–16860; 2006.
[31] Sternberg, Z.; Chadha, K.; Lieberman, A.; Hojnacki, D.; Drake, A.; Zamboni, P.; Rocco, P.; Grazioli, E.; Weinstock-Guttman, B.; Munschauer, F. Quercetin and interferon-beta modulate immune response(s) in peripheral blood mononuclear cells isolated from multiple sclerosis patients. *J. Neuroimmunol.* **205:**142–147; 2008.
[32] Darvesh, A. S.; Carroll, R. T.; Bishayee, A.; Geldenhuys, W. J.; Van der Schyf, C. J. Oxidative stress and Alzheimer's disease: dietary polyphenols as potential therapeutic agents. *Expert Rev. Neurother.* **10:**729–745; 2010.
[33] Bonen, A.; Luiken, J. J.; Liu, S.; Dyck, D. J.; Kiens, B.; Kristiansen, S.; Turcotte, L. P.; Van Der Vusse, G. J.; Glatz, J. F. Palmitate transport and fatty acid transporters in red and white muscles. *Am. J. Physiol.* **275:**E471–E478; 1998.
[34] Mertsch, K.; Blasig, I.; Grune, T. 4-Hydroxynonenal impairs the permeability of an in vitro rat blood–brain barrier. *Neurosci. Lett.* **314:**135–138; 2001.
[35] Rizzo, W. B. Sjogren-Larsson syndrome: molecular genetics and biochemical pathogenesis of fatty aldehyde dehydrogenase deficiency. *Mol. Genet. Metab.* **90:**1–9; 2007.
[36] Wildsmith, K. R.; Albert, C. J.; Hsu, F. F.; Kao, J. L.; Ford, D. A. Myeloperoxidase-derived 2-chlorohexadecanal forms Schiff bases with primary amines of ethanolamine glycerophospholipids and lysine. *Chem. Phys. Lipids* **139:**157–170; 2006.
[37] Stadelmann-Ingrand, S.; Pontcharraud, R.; Fauconneau, B. Evidence for the reactivity of fatty aldehydes released from oxidized plasmalogens with phosphatidylethanolamine to form Schiff base adducts in rat brain homogenates. *Chem. Phys. Lipids* **131:**93–105; 2004.
[38] Brahmbhatt, V. V.; Albert, C. J.; Anbukumar, D. S.; Cunningham, B. A.; Neumann, W. L.; Ford, D. A. ω-Oxidation of α-chlorinated fatty acids: identification of α-chlorinated dicarboxylic acids. *J. Biol. Chem.* **285:**41255–41269; 2010.
[39] Alexander, J. J.; Snyder, A.; Tonsgard, J. H. Omega-oxidation of monocarboxylic acids in rat brain. *Neurochem. Res.* **23:**227–233; 1998.
[40] Collins, X. H.; Harmon, S. D.; Kaduce, T. L.; Berst, K. B.; Fang, X.; Moore, S. A.; Raju, T. V.; Falck, J. R.; Weintraub, N. L.; Duester, G.; Plapp, B. V.; Spector, A. A. Omega-oxidation of 20-hydroxyeicosatetraenoic acid (20-HETE) in cerebral microvascular smooth muscle and endothelium by alcohol dehydrogenase 4. *J. Biol. Chem.* **280:**33157–33164; 2005.
[41] Pereira, A.; Braekman, J. C.; Dumont, J. E.; Boeynaems, J. M. Identification of a major iodolipid from the horse thyroid gland as 2-iodohexadecanal. *J. Biol. Chem.* **265:**17018–17025; 1990.
[42] Thomasz, L.; Oglio, R.; Rivandeira, D. T.; Dagrosa, M. A.; Jahn, G.; Pignataro, O. P.; Sartorio, G.; Pisarev, M. A. Juvenal, G. J. Inhibition of goiter growth and of cyclic AMP formation in rat thyroid by 2-iodohexadecanal. *Mol. Cell. Endocrinol.* **317:**141–147; 2010.
[43] Messner, M. C.; Albert, C. J.; Ford, D. A. 2-Chlorohexadecanal and 2-chlorohexadecanoic acid induce COX-2 expression in human coronary artery endothelial cells. *Lipids* **43:**581–588; 2008.
[44] Fernandez-Hernando, C.; Fukata, M.; Bernatchez, P. N.; Fukata, Y.; Lin, M. I.; Bredt, D. S.; Sessa, W. C. Identification of Golgi-localized acyl transferases that palmitoylate and regulate endothelial nitric oxide synthase. *J. Cell Biol.* **174:**369–377; 2006.
[45] Knott, A. B.; Perkins, G.; Schwarzenbacher, R.; Bossy-Wetzel, E. Mitochondrial fragmentation in neurodegeneration. *Nat. Rev. Neurosci.* **9:**505–518; 2008.
[46] Landar, A.; Zmijewski, J. W.; Dickinson, D. A.; Le Goffe, C.; Johnson, M. S.; Milne, G. L.; Zanoni, G.; Vidari, G.; Morrow, J. D.; Darley-Usmar, V. M. Interaction of electrophilic lipid oxidation products with mitochondria in endothelial cells and formation of reactive oxygen species. *Am. J. Physiol. Heart Circ. Physiol.* **290:**H1777–H1787; 2006.
[47] Boveris, A.; Chance, B. The mitochondrial generation of hydrogen peroxide: general properties and effect of hyperbaric oxygen. *Biochem. J.* **134:**707–716; 1973.
[48] Usatyuk, P. V.; Natarajan, V. Hydroxyalkenals and oxidized phospholipids modulation of endothelial cytoskeleton, focal adhesion and adherens junction proteins in regulating endothelial barrier function. *Microvasc. Res.* **83:** 45–55; 2011.
[49] Haorah, J.; Ramirez, S. H.; Schall, K.; Smith, D.; Pandya, R.; Persidsky, Y. Oxidative stress activates protein tyrosine kinase and matrix metalloproteinases leading to blood–brain barrier dysfunction. *J. Neurochem.* **101:** 566–576; 2007.
[50] Haorah, J.; Knipe, B.; Leibhart, J.; Ghorpade, A.; Persidsky, Y. Alcohol-induced oxidative stress in brain endothelial cells causes blood–brain barrier dysfunction. *J. Leukocyte Biol.* **78:**1223–1232; 2005.
[51] Butt, O. I.; Buehler, P. W.; D′Agnillo, F. Blood–brain barrier disruption and oxidative stress in guinea pig after systemic exposure to modified cell-free hemoglobin. *Am. J. Pathol.* **178:**1316–1328; 2011.
[52] Mitchell, R. W.; Edmundson, C. L.; Miller, D. W.; Hatch, G. M. On the mechanism of oleate transport across human brain microvessel endothelial cells. *J. Neurochem.* **110:**1049–1057; 2009.